Type Ia Supernovae "Orphans": A Window on Cosmology

James A. Schlaerth

Thesis for Honors in Astronomy

Department of Physics and Astronomy
Vanderbilt University
Nashville, TN

Abstract

We report on cosmological implications for Ω_M and Ω_Λ from measurements of type Ia supernovae fluxes taken by the Supernova Cosmology Project on observing runs between fall 1997 and spring 2001. The observed images of the supernovae were calibrated based on stars in each image, and had reference images subtracted to obtain correct supernova flux measurements from several different points during the life of the supernova. From the flux measurements typically over a 2-month period, a lightcurve, or flux vs. time relationship, could be fitted to an empirically known template derived from low-redshift supernovae. The supernovae are then K-corrected to fit into the rest-frame B and V filters with the correct colors, and corrected for time dilation effects on the lightcurve delay. From these steps, we can estimate the true peak luminosity and the stretch, a measure of the decay rate of the supernova flux, to use the supernova as a "calibrated candle" to measure cosmological parameters. Our results, completely independent of any other high-redshift surveys, strongly agree with the results of Perlmutter el al. (1999) and Knop et al. (2003) in ruling out an "Einstein-de-Sitter" universe ($\Omega_M = 1$, $\Omega_\Lambda = 0$) and are consistent with measurements for a positive cosmological constant. Assuming a flat universe, this independent data set provides a best-fit measurement of $\Omega_\Lambda \approx 0.68$, completely consistent with the original SCP data.

Chapter 1: Introduction

The idea of "standard candles" used for use in cosmology has always been present with the need to determine distances to far-away objects. This idea has become most attractive since the discovery of Hubble expansion, when it was determined that the redshift, z, of a galaxy showed how much space had expanded since the light was emitted. A "standard candle" could then give you the distance to the galaxy, and you could create a graph of distance vs. expansion rate of the universe to each. This would be instrumental in telling you the expansion rate of the universe and, more importantly, if the expansion rate is constant. However, until the use of type Ia supernovae as a type of "standard candle" by the Supernova Cosmology Project (SCP) and the High-z supernova search team, there was no good method of finding this relationship at high redshifts ($z > 0.3$) probed in this paper.

The idea behind the Supernova Cosmology Project is relatively simple: knowing the peak magnitude and the "stretch," a quantity dependent upon the decay rate of the luminosity of the supernova, one can calculate at what distances the supernova should be to match the observed properties of nearby supernovae. These values of luminosity distance versus redshift are well-known for several types of universes, particularly for flat, matter-dominated universes and for flat, accelerating universes.

Cosmology and Cosmography

It is helpful to first understand the units used by astronomers to measure the flux from an object on a large scale. The definition of magnitude is

$$m=-2.5 \log (f) + \text{constant} \tag{1}$$

where f is the flux and the constant is a conventionally adopted value. The absolute magnitude simply tells us what flux we would perceive if the source were 10 pc (32.6 ly) away. We can then define the distance modulus as

$$m-M=-5\log\left[\frac{d}{10\,pc}\right] \quad . \tag{2}$$

Thus we can tell the distance to any object whose absolute magnitude is known.

In cosmological studies, one must first define some parameters (e.g., Hogg 2000). The redshifted light is entirely due to the expansion of the universe, and the redshift z is defined as

$$z\equiv\frac{\lambda_{observed}}{\lambda_{emitted}}-1=\frac{\nu_{emitted}}{\nu_{observed}}-1 \quad . \tag{3}$$

This redshift determines the "scale factor" of the universe, or the ratio of the universe's size at different times:

$$1+z=\frac{R(t_{observed})}{R(t_{emitted})} \quad . \tag{4}$$

The value which describes the expansion rate of the universe is known as the Hubble parameter H(t), which currently takes a value H_0, the Hubble constant. It is defined by

$$H(t)=\frac{dR/dt}{R} \quad . \tag{5}$$

R is given as the relative size for the universe, which currently takes on a value of R_0. For low redshift objects, a good approximation is to say that $v = H_0\, d_L$, where v is the observed recessional velocity and d_L is the distance to the object.

With these values defined, we can now take the tested results of general relativity on faith (as I myself have not attempted to derive them yet), and trust the Friedman-(Lemaître)-Robinson-Walker metric. This shows that the universe must be expanding at a decelerating rate or even contracting in the case of no cosmological constant, but could expand at an accelerating rate with the cosmological constant. The Friedman equation is written as

$$\left[\frac{dR}{dt}\right]^2-\frac{8G\rho R^2}{3}-\frac{\Lambda R^2 c^4}{3}=-kc^2 \tag{6}$$

or

$$H^2=\frac{8\pi G\rho}{3c^2}-\frac{k}{R^2}+\frac{\Lambda c^2}{3} \tag{7}$$

In these equations, ρ is the mass density of the universe and k is the universe's curvature. The cosmological constant, Λ, was introduced by Einstein to balance gravity and produce a static universe, but can be used to accelerate an expansion as well. The constant arises naturally out of the equations, and is the simplest means of justifying any observed acceleration. A spatially flat universe (k=0) would yield two important densities which would add up to 1, $\Omega_\Lambda = \Lambda/3H_0^2$, and $\Omega_M = \rho/\rho_C = 8\pi G \rho /3H_0^2$, where ρ_C is defined to be the "critical density" of the universe. The values for Ω_M, ρ and ρ_C are all the present-day values. When the total energy density of the universe is equal to ρ_C, the geometry of the universe is spatially flat. The existence of a cosmological constant would mean that the universe could be accelerating after an initial deceleration, and would be measurable with the existence of type Ia supernovae as standard candles. The nature of the "dark energy" that would cause such acceleration is unknown, as pure vacuum energy would prove 120 orders of magnitude too large (Carroll, Press and Turner 1992)

Type Ia Supernovae

In our measurements of Ω_M and Ω_Λ, we must also deal with two separate "nuisance" parameters, $\mathcal{M}$ and α. The α parameter corrects for a small dependence of intrinsic supernova luminosity upon the decline rate of the supernova, measured with the stretch parameter *s*. $\mathcal{M}$ comes about because our flux measurements are made to be independent of both H_0 and the true supernova absolute magnitude. The parameters $\mathcal{M}$ and α are primarily determined by low-redshift supernovae, while the higher redshift supernovae provide a greater test for the values of Ω_M and Ω_Λ. The full equation for the magnitude of a type Ia supernova in the B band is

$$m(z) = M + 5 \log cz - 5 \log H_0 + 25 - \alpha (s-1) \qquad (8)$$

where M is the absolute magnitude of the supernova (the magnitude if it was observed from 10 pc), and the 25 arises as a factor for converting units of H_0 from Mpc to a distance of 10 pc. We take the "Hubble constant free" Magnitude $\mathcal{M}$ to be defined as

$$\mathcal{M} = M - 5 \log H_0 + 25 \qquad (9).$$

Thus the distribution of supernovae no longer depends explicitly upon H_0 and we need not bother using the exact measurements to find the true flux expected from a s=1 supernova.

When completely corrected, we have a much simpler version of the equation for corrected B magnitudes

$$m_B = \mathcal{M} + 5 \log \mathcal{D}_L (z; \Omega_M, \Omega_\Lambda) - \alpha(s-1) \qquad (10)$$

where $\mathcal{D}_L = H_0 d_L$, the "Hubble constant free" luminosity distance (Perlmutter et al. 1997), and $d_L = (L/4f)^{1/2}$. This value of m_B is seen plotted on the graphs and depends only upon the parameters listed. Thus, it is an effective probe of the densities Ω_M and Ω_Λ, which determine the expected values for m_B for a given redshift once all other parameters have been eliminated, or summed over. The plots of magnitude versus redshift seen in the results in Figure 9 come from this equation.

Interpretation of Apparent Brightness

In our data, we are able to find an effective brightness for any given supernova, and plot it on what is expected for a certain redshift. The dimmer the supernova is measured to be, the more the universe is accelerating in its expansion, and the bigger the measured value for cosmological constant Λ. The reasoning behind this is not necessarily straightforward. When the SCP measures the flux of a given supernova, assumed for simplicity to be a true standard candle, we are actually measuring the true distance to that supernova. The distance we get from measuring the flux is a measure of lookback time; due to the finite speed of light, the farther something is, the greater the lookback time. The redshift of the supernova observed is a measure of the amount of cosmic expansion between when the light was emitted and today. A dimmer supernova for a given redshift means that it took longer for expansion to get to this point, meaning expansion must have been slower in the past than it is today. Therefore, the dimmer the supernovae at high redshift, the greater the acceleration rate of the universe. In principle, there should be a turning point at $z \sim 1$ at which time the initial deceleration period (before the hypothesized "dark energy" overcame the mass density of the universe to begin acceleration) yields supernovae brighter than otherwise expected, but this is well beyond the largest redshift in this paper.

Chapter 2: The Supernova Cosmology Project

The Supernova Cosmology Project started looking for supernovae by subtracting images to look for changes in brightness of incredibly dim galaxies which correspond to supernovae. Beginning in the early 1990s, the group began taking long exposures to look for cosmologically significant supernovae. This is done primarily by the process of surveying wide areas of the sky over several nights, then returning to survey the same sky areas some time later. Supernovae must, therefore, be seen from a telescope with a wide field of view, so before the installation of the Advanced Camera for Surveys (ACS) in 2002, the Hubble Space Telescope (HST) was not a good tool for wide field searches. Given the extremely faint supernovae, long observations must be taken to clearly identify the supernovae over the background. This calls for long exposures – approximately 5-60 minutes on a telescope such as the CTIO 4-meter – to get reasonable signal-to-noise ratios for the supernovae, which generally have apparent magnitude of the order of 23rd R-band magnitude (about 10^{-8} times the flux from the sun at 10 pc / 32.6 ly in R band) for $z \sim 0.5$. Usually observations must be scheduled for the time of the month when the scattered sky background light from the moon is least. The initial images are subtracted from images taken roughly a month later, and prospective supernovae are followed up on subsequent observations. The search fields are generally observed on several consecutive nights to make sure that other objects, such as asteroids, cannot be confused with supernovae. In general, these are eliminated in follow-up images, and only supernova events of all kinds, with a few contaminants such as active galactic nuclei, remain. The events are ideally observed for several weeks to measure the complete decline of the supernovae in order to make the best possible estimate of the lightcurve shape and flux.

The best candidates are also observed spectroscopically, usually at the Keck 10 meter telescopes in Mauna Kea or at the ESO 8 meter Very Large Telescope in Chile. Most are confirmed type Ia supernovae through absorption lines in the spectrum, while a few are determined only through photometry (which includes a surprisingly high percentage of the supernovae I was working on, known as the "orphans"). The redshift is also determined here as long as the spectrum has low enough noise to clearly distinguish lines. The redshift is generally determined from the galaxy, but the Ia spectra are known well enough to determine redshift from that alone. When a template galaxy spectrum is subtracted, the lines generally become clear enough to confirm the SN type.

The results of the SCP, whose data are being used for this independent set of supernovae, are obtained from ground-based telescopes in a sample of 42 supernovae (Perlmutter et al. 1999, hereafter P99) and from primarily HST in a sample of 11 supernovae (Knop et al. 2003, hereafter K03). In these papers, the collaboration developed the procedure used in this project to find the total flux of a given supernova, fit it to a template lightcurve of a type Ia supernova, and draw cosmological conclusions based on the data extracted. Each data set is combined with information from the much better lightcurves of the low redshift supernovae to get similar probability distributions for M and α.

The competing collaboration, the High-z supernova search team, has independently obtained results consistent with those presented by the SCP. Using independent methods for luminosity determination of supernovae, there is good agreement upon the highest probability for the value of the cosmological constant. The next step for the SCP is to use the proposed Supernova Acceleration Probe (SNAP satellite) to detect thousands of supernovae out to z~1.7 in order to map the expansion history of the universe much better than is presently possible, and to probe the properties of dark energy.

The supernovae presented in this project belong to a group of 39 observed supernovae not released in either P99 or K03. These "orphans", called this because of their failure to be included with the supernovae in published papers, have been detected between fall of 1997 and spring of 2001. Most have spectroscopic data and determined redshifts, including spectroscopic confirmation of being type Ia supernovae. However, many of these supernovae have only R-band data, or have other flaws in the data (see Appendix A for a thorough analysis of each supernova).

Chapter 3: Determination of Brightness

The flux measured from a supernova is found simply by subtracting a "reference" image, taken about a year later, from a "new" image, an image containing a supernova as it explodes. Whatever is left over is the observed flux from the supernova. To do this subtraction properly, one must go through complexities of finding the exact location of the supernova, finding how much of the light observed at the position of the supernova is from the host galaxy, and calibrating different images to ensure correct subtraction.

To understand the calibration and flux measurements taken from different telescopes, we must define two types of nearby objects seen on each CCD image containing a supernova: the "fiducial objects" and the "secondary standard stars." The fiducial objects are primarily background galaxies similar to the ones containing supernovae, and are used primarily in determining the flux from a supernova on a given image. The secondary standards are stars in the Galaxy with no companions visible out to approximately 4 FWHM, and are used primarily for relative calibration between images.

Subtraction and Flux Measurements

The first step in the subtraction process is to choose the 10-15 best reference images, containing no supernova light, with the best seeing (effective angular resolution) and signal-to-noise ratio. These "ref" images are all subtracted from the "news" to get the best possible value for the supernova flux from each "new" image. Thus, one really gets 10-15 different values for the flux at any given point, and the variance-weighted average of those is the value recorded on the lightcurve. Several steps must be taken to get the final value for the flux at a given point from this subtraction, including accounting for seeing and finding the exact position of the supernova.

For a given point source, which supernovae are, one must take into account the "point spread function" (psf), which comes from the fact that a point source will be detected to have a certain width on a telescope of finite radius. If all images came from a space-based telescope, this would be the only blurring to account for. However, the atmosphere of the Earth distorts the incoming wavefront of light from the supernova, and we see a much more spread-out blob of light, the "seeing disk", the size of which depends on the observing conditions. The worse the seeing, the more spread-out the supernova will appear to be.

Each image taken of the host galaxy, with or without the supernova, has a different value for seeing. One could not simply subtract two images with different seeing, as this would lead to an incorrect value for the flux. Therefore, during subtraction, the image with better seeing is blurred to match the other image, so that the point spread function of the supernova is all that will remain after subtraction, with no galactic light as a side effect from the blurring.

Finding the exact central location of the supernova is necessary in order to maximize the efficiency and the accuracy of the supernova flux measurement. The centroid of the distribution of flux left over from subtraction is used to determine where the supernova is located. In general, this results in a plot with numerous points in and around a central area differing on the order of a pixel. The "news" with little supernova flux are not considered in position-finding. An average value of the centroids from the fits as well as a standard deviation are found. These are then used as the position of the supernova for another subtraction, where the centroid of the subtracted flux is again used to find a new position. The recentering process goes through many iterations, until the center of the supernova agrees with the center in the previous iteration to within a fraction of the uncertainty. At this point, we can be sure that we are measuring the supernova with an aperture centered on its position, and the error in flux based on position becomes negligible compared to other systematic uncertainties.

After correcting for position and seeing, we can concentrate on ways to best reduce host-galaxy light contaminating the supernova measurement, and how to find the errors in supernova flux. The fiducial objects, mentioned above, provide both a measure of the errors in flux measurement and a test of the host galaxy's contribution to each image. First, the ratios of the fiducials between "news" and "refs" gives the factor by which the "ref" must be scaled such that, during subtraction, all the host galaxy light is subtracted.

Second, the dispersion in the flux of the fiducial objects on “new” images, when “ref” images are subtracted, allows the computation of the standard deviation of magnitudes on a given point. The greater the variance about zero flux of the fiducials the larger the error bar becomes. In practice, all these steps with the fiducial objects happen at once to allow the most precise subtraction.

Relative Calibration

In order to determine the true flux from the supernova, we must take into account the “zero point magnitude” m_{ZP} to put our CCD measurements on a calibrated system. This is factored in by the equation

$$m_{app} = -2.5 \log (f) + m_{ZP} - bx \tag{11}$$

where m_{app} is the apparent magnitude, f is the flux and bx is the “airmass” term. In the bx term, x is approximately equal to the secant of the zenith angle, and b is of the order 0.1. There is also a correction for colors seen through different telescopes, which normally results in a change on the order of 0.01 magnitudes.

Determining the exact value for the zero point itself cannot be done by simply looking at the field containing the supernova. To determine the value of m_{ZP}, each observing run ideally looks at several fields of standard stars throughout the night (Landolt 1992). These stars of known and constant brightness can be used, given their measured flux on a given night, to find the zero points for observations that night. These zero points are used to measure the magnitudes of “secondary standards” in images of the supernova field taken on the calibrated night. Several calibrated nights are used rather than having calibration from each run, as this can only be done on consistently clear nights when calibration data is taken. The secondary standards are then used to relatively calibrate each supernova observed at different epochs.

Supernovae are measured only out to a radius of one FWHM so that the signal-to-noise ratio of the supernova remains high. The secondary standards are used to correct the supernova to an infinite aperture. The aperture correction must be measured on other point sources, which the secondary standard stars are, in order to get the same distribution. Because the aperture correction should be the same for a point-source supernova as for a star with no nearby companions, we can use this to correct the supernova.

In addition to these calibration techniques, we must account for the correlated errors between photometric data points due to the fact that the same refs are used for each new image. Thus, all the points on the lightcurve will have some correlation in the error bars, which is accounted for with an error matrix.

For several supernovae in this set of “orphans”, data was taken during my senior thesis during an observing run at Cerro Tololo’s 0.9 meter telescope in La Serena, Chile. These supernovae had little to no calibration data before, and thus it was crucial to the correct determination of their flux that extra data be taken. Many of the supernovae observed in 2001 lacked any calibration data at all, and thus it was impossible to include many of these in the thesis. Unfortunately, the data came in too late to be used in this thesis, but it will be processed by the successor on this project.

Extinction and Reddening

Extinction is the absorption of light emitted from astrophysical objects by dust in between the source and the telescope. There are two types of extinction to take into account for extragalactic observations: Galactic extinction (light absorbed by dust in the Milky Way) and host-galaxy extinction, light absorbed by dust in the galaxy containing the observed supernova. Dust from the host and the Galaxy preferentially absorb shorter wavelengths, a process called reddening. The color excess values due to reddening, E(B-V), are determined by the function

$$E(B-V) \equiv (B-V)_{observed} - (B-V)_{true} \tag{12}$$

where

$$B-V = -2.5\log\left(\frac{f_B}{f_V}\right) + const \quad . \tag{13}$$

In these equations, B and V are magnitudes for the blue and green bands, respectively, and B-V is a color. The greater B-V is, the redder the object. Reddening is understood for each band, where the extinction, A_X (extinction in whatever X band is used), divided by the amount of reddening will yield a roughly constant value, R_X. The standard value for the ratio, R= A_X/E(B-V), in the B band will be approximately 4.1, and in the V band the value will be about 3.1, according to the extinction law discussed in Cardelli, Clayton and Mathis (1989) . Both host-galaxy and Galactic extinction and reddening must be accounted for in order to find the true flux coming from the supernova. Extinction from the Galaxy is low along the line-of-sight used, and is corrected for using the extinction law of Schlegel et al. (1998).

One can make the heuristic argument, supported by simulations of host-galaxy dust extinction and by previous observation, that the supernovae we see would be extincted very little by dust. This occurs because of one of two possibilities. First, the supernova could be in an elliptical host galaxy, where there exists little to no dust. Second, though, it could exist in a dust filled galaxy, in a flux-limited survey we would not find a supernova that was heavily extincted. The average scale height of type Ia supernovae above the galactic plane in a spiral galaxy is high for type Ia supernovae (Hatano, Branch and Deaton 1998, hereafter HBD98), leading to two possible scenarios: Either the supernova is behind a large amount of dust in a spiral galaxy, where a flux-limited survey is unlikely to detect such a supernova, or it is on the near (to us) side of the disk of the galaxy and is not heavily extincted. This is particularly true at higher redshifts, as the supernova flux decreases with distance, making it hardest to find extincted supernovae at the largest redshifts.

For most supernovae in a high redshift sample, the evidence that extinction must be either negligible or very little has been found both in simulation (HBD98) and in observation (K03). In HBD98, models of host galaxy extinction were used to determine the probability of values of A_B, B-band host galaxy extinction, for a typical spiral galaxy face-on, edge-on, and at random inclinations to us. Supernovae were simulated to be near the galactic bulge and in the more cool-gas-filled disk area, where supernovae are a factor of 7 more common. The probability function for host galaxy extinction levels is seen in Figure 2, and shows that for any distribution the probability density becomes greatest at values of $A_B \leq 0.1$ for both bulge and disk supernovae.

HBD98, however, says nothing about a flux limited survey, as the probability of A_B just shows the amount extincted to any nearby observer. We must account for the probability that an observer from Earth is much less likely to find a supernova with host galaxy extinction A_B~0.5 than one with A_B<0.1. With 10 minute images taken from telescopes such as the CTIO 4-meter, a heavily extincted supernova in the Earth-frame R band is much less likely to be pursued after initial resubtraction than one at the same redshift with little or no extinction. Riess et al. (1998) used HBD98 by applying a one-sided function of E(B-V) to their data and found it to give roughly 50% of the data an extinction of E(B-V)=0, with probability decreasing exponentially to higher extinction levels.

Evidence in support of this has been clearly outlined in papers presenting data from previous SCP searches, most notably K03, in which supernovae were corrected for extinction. The eleven HST observed supernovae in that paper show an initial scatter of extinction at low redshift and consistency near zero as redshift increases beyond z~0.5. All data seems to support the assumption made above, and therefore supernovae with only one band of data are included in the final results of this paper.

Chapter 4: K-corrections and Lightcurve Fitting

Once we have measured the supernova lightcurve, the graph of flux versus time, we can fit a template lightcurve to it to find the peak magnitude to serve as a standard candle (see Figure 1). The lightcurve shape involves two parameters crucial to cosmological fitting: the "stretch" of the lightcurve and the peak magnitude. It is shown by Goldhaber et al (2001) that these two parameters are all that is needed to calibrate a supernova's flux and use it as a standard candle at cosmological distances.

Fitting the Empirical Lightcurve

Due to the abundance of low-redshift Ia supernovae detected, the lightcurve shape is well known empirically, and thus relatively simple to fit. It has been observed from many low-redshift supernovae that, the greater the luminosity of the supernova, the longer the decay time and, therefore, the greater the stretch parameter. This is why type Ia supernovae cannot be considered “standard candles” in the true sense of the word, but rather “calibrated candles.”

The stretch-luminosity relation for a type Ia supernova at redshift z=0 is empirically described by the equation

$$m_B^{corr} = m_B + \Delta_{corr}(s) \quad (14)$$

where

$$\Delta_{corr}(s) = \alpha(s-1). \quad (15)$$

Thus, it is easy to see that as s becomes less than 1, the $\Delta_{corr}(s)$ becomes negative. Thus, the correction makes the observed m_B brighter to correspond to the brightness of a supernova with a stretch of 1. The parameter α is empirically found to be approximately 1.5, from plots of $\mathcal{M}$ vs. α in previous groups of supernovae. The confidence regions for $\mathcal{M}$ and α from this subset are found in Figure 5, from which we can find the maximum probability for α.

Along with considering intrinsic stretch to fit the supernovae, one must consider the effects of cosmological time dilation based on redshift. This gives us another factor of (1+z) which must be applied to the time axis in addition to the stretch. Therefore, we define a parameter width, $w \equiv s(1+z)$, which normalizes the lightcurve decay timescale to what it would be at redshift z=0 (Goldhaber et al. 2001).

The actual fitting of the data points by the lightcurve is done by the MINUIT program (James & Roos 1994). The program fits a function, normalized to the peak flux, consisting of a parabolic rise to maximum light, an empirical curve during the first phase of the supernova's decay, and an exponential tail (Goldhaber et al. 2001). An example of this fit to a supernova is shown in Figure 1. It is shown that this template fits the low-redshift data to a χ^2/DoF ~ 1, with the only three parameters needed to fit the graph being the peak flux, the stretch, and the time of maximum light. Once stretch is corrected for, the supernova essentially becomes a true "standard candle."

In all, the typical stretch of a type Ia supernova varies between s=0.7 and s=1.3, making it possible to weed out many type Ibc and II supernovae which may corrupt the data sample. The uncertainty in absolute B magnitude for a variance in stretch this large is 0.45 magnitudes for α = 1.5. In practice, however, we seldom see these extremes in stretch, so an uncertainty in magnitude of 0.15, the uncertainty considering values between s=1.1 and s=0.9, is much more likely. This makes stretch a somewhat important factor, but much less than peak magnitude.

For those supernovae with enough data points, particularly during the decay of the lightcurve, it is easy to measure the stretch of the supernova from these fits. However, in some cases, few data points were known, and the stretch was fixed to the median stretch of 1.0. If the stretch is somewhat uncertain, there will also be great uncertainty on the graph of magnitude vs. redshift. This was particularly the case with sn9827 and sn9869, whose uncertainty of stretch contributed to much larger error bars (see Figure 9).

Several of the supernovae have only 2 to 4 images available, and thus a lightcurve fit which included the stretch would be simply impossible to make. In addition, if the time of maximum was not known, one could not determine the luminosity of the candidates. However, some of these supernovae had spectra taken. Due to the characteristic spectra of type Ia supernovae, one can in principle determine the time of maximum of the supernova, and thus find the approximate peak luminosity of the supernova. The process of determining "snapshot distances" to supernovae is detailed in Riess et al. (1997). Several of the supernovae used in this search had such problems, but few had spectra with good enough data to determine the time or the stretch. In addition, those candidates for the "all in one night's work" procedure described by Riess et al. contained only R band images. These candidates were either fitted with a fixed stretch, as in S01-078, or left out, as in S01-029 (due primarily to redshift uncertainty - see Appendix A).

K-Corrections to Rest-Frame Wavelengths

After fitting the lightcurve, K corrections must be made in order to transform observed R-band light into its rest-frame B-band for supernovae of $0.3 < z < 0.7$. This is seen from the equation

$$m_B^{eff} = m_R - \alpha(s-1) - K_{BR} - A_R \tag{16}$$

where K_{BR} is the K-correction term from observed R-band to B-band. The de-redshifted R-band does not match perfectly to the rest-frame B-band (see Figure 6), so we must include a correction from the area covered in the R-band. Therefore, there is a small additional uncertainty of the zero points in the rest-frame band.

Chapter 5: Cosmological Results

The results found in this project alone rule out an "Einstein-de-Sitter" universe to high confidence, and show good agreement with previous studies by the SCP and High-Z supernova search team. The most thorough view of this is seen in the plot of confidence regions of Ω_M vs. Ω_Λ (Figure 7). This graph shows the intervals at 68%, 90%, 95%, and 99% confidence of the values of the two parameters. The minimum χ^2 value for any plot is 42.2 with 32 supernovae, or χ^2/DoF =1.3, for a universe with the values $\Omega_M = 1.07$ and $\Omega_\Lambda = 1.60$. Obviously, this χ^2 is not ideal, but is still acceptable given the number of supernovae presented. The individual probability distributions of Ω_Λ and Ω_M are shown in Figures 3 and 4, respectively.

This is not a good method of determining the amount of matter in the universe or finding an exact value of the cosmological constant independently; however, by itself, it indicates a positive cosmological constant to high confidence. In this plot, the "Einstein-de-Sitter" universe is ruled out to greater than 99% confidence, and the probability for a positive cosmological constant is approximately 98.9%.

One can still see that a flat universe is well within the probability values on this graph. Because a flat universe ($\Omega_M + \Omega_\Lambda = 1$) is suggested by CMB data, we will consider the most probable values for a flat universe as well. It is within the 68% confidence interval, and is thus fully permitted by the data. The probability for Ω_M and Ω_Λ in a flat universe is shown most clearly when looking at the confidence regions in Figure 8. This graph is essentially a section or cut through the probabilities in Figure 7. It shows that, if the universe is constrained to be flat, the amount of matter in the universe is most probably $\Omega_M = 0.32$, implying a cosmological constant of $\Omega_\Lambda = 0.68$.

In Figure 9 are plotted the individual data points, complete with error bars corresponding to stretch and peak magnitude uncertainties from photometry. One can tell from this plot that the $\Omega_M = 0.3$ and $\Omega_\Lambda = 0.7$ universe is the best fit of the three possibilities. This is shown most clearly when looking at the confidence regions in Figure 7, where the probability for an $\Omega_M = 0.3$ and $\Omega_\Lambda = 0$ universe is ruled out to at least 95% probability.

The values of maximum probability for $\mathcal{M}$ and α, heavily weighted to the low-redshift supernovae also used in the previous searches, are $\mathcal{M} = -3.49 \pm 0.05$ and $\alpha = 1.52 \pm 0.20$. The probability distribution (Figure 5) is well within the range of previous supernova searches by the SCP.

References

Cardelli, J. A., Clayton, G. C., & Mathis, J. S. 1989, ApJ, 345, 245

Carroll, S., W. Press, & E. Turner, "The Cosmological Constant", ARAA, 30, 499 (1992)

Goldhaber, G., et al. 2001, ApJ, 558, 359

Hatano, K., Branch, D., & Deaton, J. 1998, ApJ, 502, 177

Hogg, D. 2000, Astro-ph, 9905116

James, F., & Roos, M. 1975, Comput. Phys. Commun., 10, 343

Knop, R et al., 2003, ApJ, 598, 102 (K03)

Landolt, A. 1992, AJ, 104, 340

Perlmutter, S. et al., 1999, ApJ, 517, 586 (P99)

Perlmutter, S. et al., 1997, ApJ, 483, 565

Riess, A. et al., 1998, ApJ, 504, 934

Schlegel, D. J., Finkbeiner, D. P., & Davis, M. 1998, ApJ, 500, 525

APPENDIX A

Supernovae Explanations of Data Points, from the 39 objects considered.

Included Supernovae

sn97188: This supernova is one of the better ones, well-behaved at a redshift of 0.633 from galaxy features. It is a probable type Ia spectroscopically, with weak supernova features which become more clear with a template galaxy subtracted. Overall, it is one of the better supernovae of the bunch.

sn97190: This is a low-redshift supernova at z=0.361, spectroscopically confirmed with clear features.

sn97195: This is also a spectroscopically confirmed type Ia at redshift 0.466, measured from both the galaxy and the supernova.

sn97203: A confirmed supernova at z=0.46, this supernova could have some reddening, explaining its location as too high for the fit of $\Omega_\Lambda \sim 0.7$

sn97227: This has a "beautiful" type Ia spectrum and redshift 0.498. It is another of the best supernovae with plenty of datapoints in each band.

sn9827: The stretch is somewhat uncertain, as evidenced from the large errors in figure 11. It is an unconfirmed type Ia which seems to fit a lightcurve well (chi-square less than 1). It is only observed in the R-band, and therefore has unknown extinction. The redshift of 0.62 is determined from galaxy lines. This is possibly the most uncertain of all the included supernovae, with no datapoints during the decline in brightness.

sn9869: Also observed only in the R-band, this supernova has a slightly more certain stretch, and also fits a lightcurve plot at a chi-square better than 1. The stretch is somewhat uncertain, with only one data point on the decline. The redshift of .507 is determined from nearby galaxy lines, with no clear supernova features.

sn98149: This supernova, also only seen in the R-band, is a confirmed type Ia spectroscopically with the redshift 0.410 determined from galaxy lines. It is another good candidate which would benefit from I-band data.

S01-033: This is one of the best supernovae, but at a modest redshift of 0.36. It is spectroscopically confirmed with supernovae lines, fitting very well into the plot.

S01-077: This supernova is only observed in the R-band, but is a clear type Ia at z=.511 from spectroscopy of galaxy lines. A good supernova, but generally lacking in data points, with only five during the peak times.

S01-078: Much like S01-077, this one is observed only in R-band during its peak brightness. With fixed stretch, it is found to have a redshift of 0.58 and probably galaxy lines from spectroscopy.

Supernovae Not Included:

S01-004: Due to the loss of images in hardware malfunctions at Berkeley, this could not be included.
S01-017: This supernova is also missing some images in its lightcurve due to the Berkeley problems.
S01-028: If the spectrum showed anything, this would be a possible "all in one night's work" candidate, but as it is there is nothing to go on. There is very little chance of learning anything from this supernova, only observed in the R-band.
S01-029: This is one of the more interesting cases. There are only about three points, which are all in the R-band, and getting a stretch or peak magnitude out of it is impossible. In addition, the spectrum was so noisy that the redshift was narrowed down to two values: 0.37 and 0.56. There seems little hope for finding anything cosmologically significant from this supernova.
S01-031: This supernova is missing over a third of its images from Berkeley.
S01-034: The hardware problems cost this supernova its primary reference, meaning I cannot continue.
S01-048: Perhaps the least cooperative of the supernovae with missing images, this one had too many problems to pursue.
S01-054: Hardware problems, like almost all S01's.
S01-065: Missing images plague this one as well.
sn97180: This supernova is very nice looking supernova in R band, but I band points seem to be very high for such a fit. This yields a total chi-square value of over 2.0, and a great suspicion that this supernova is reddened.
sn97192: This has a low brightness and high stretch ($s \sim 1.4$) suggesting that it is a core-collapse supernova.
sn97193: As an unconfirmed type Ia supernova, this has a stretch too high ($s > 1.3$) to be considered a type Ia. It is also too dim and therefore a probably core-collapse supernova.
sn97218: This supernova, unconfirmed spectroscopically, had a stretch ~1.4 too large to be considered a type Ia.
sn97234: This supernova does not have much of a lightcurve, and it cannot be determined if this is a supernova, let alone a type Ia.
sn9841: This could be a good candidate, but has no spectroscopic information. It was only observed in the R-band.
sn9849: This could be a good candidate, but has no spectroscopic information. It was only observed in the R-band.
sn9853: This could be a good candidate, but has no spectroscopic information. It was only observed in the R-band.
sn9857: This could be a good candidate, but has no spectroscopic information. It was

only observed in the R-band.

sn9884: This is clearly a supernova, and clearly not a type Ia. The flux is much too low for any redshift. This one is easily thrown out.

sn9898: Only observed in the R-band, this supernova has no stretch information and no confirmed time of maximum. Without any spectroscopic information, other than identification as a "probable Ia", nothing can be done.

sn98138: With no spectroscopic confirmation and overall bad data points, there is no way to include this supernova.

sn98141: This could be a good candidate, but has no spectroscopic information. It was only observed in the R-band.

Other Objects:

sn98140: This object, clearly not a supernova, is probably an AGN because of its brightness over a year later. It was observed by HST, which now seems like a waste.

sn98144: This object is most probably an AGN, as it was brighter one year later than it was when supposedly a supernova.

sn98147: It has not yet been determined why exactly the SCP decided to follow this object, as it does not seem to be an AGN or supernova. It is best labeled "junk."

Recently included, delayed due to hardware problems:

sn97216: This supernova looked good, with R and I band, and had no significant difficuties.

Sn97241: This supernova had some major difficulties during K-corrections, as the I-band data is terrible. All iterations lead to the belief of the color as R-I ~ -6.0. This is obviously wrong, and therefore it could not be included in the data.

sn98114 (R-band only): Aside from not having any I-band data, this was a very good supernova with good data. It was easily included in the revised draft.

APPENDIX B

Pictures and Graphs

Figure 1: An example of an R-band lightcurve, of supernova 98149, with data points summed over all images taken in a given night. This is one of the clearest supernovae, at a redshift of 0.46. The peak flux is normalized to 1.

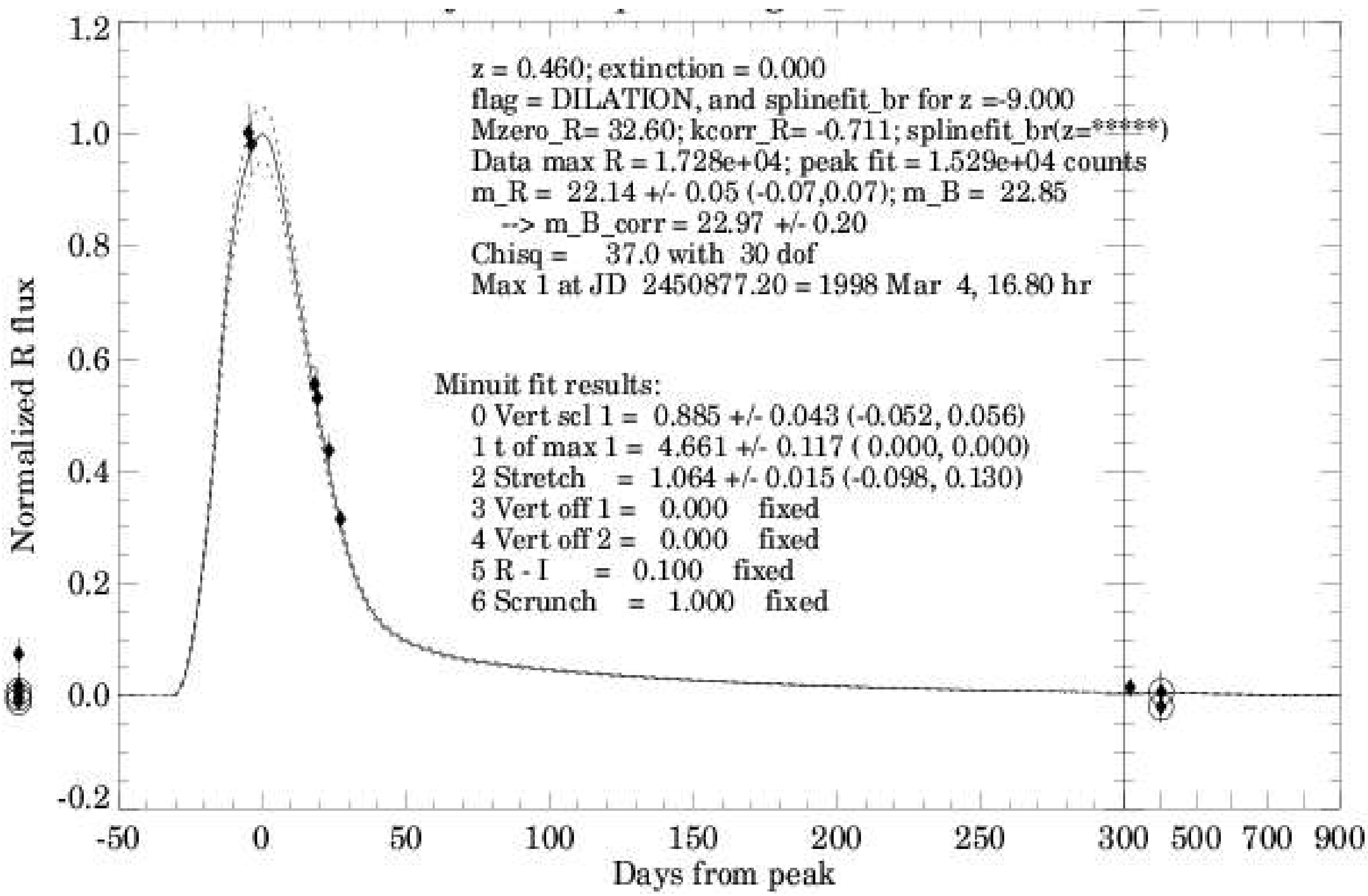

Figure 2: The probability of extinction A_B for (a) bulge supernovae, (b) disk supernovae and (c) Type II supernovae based on simulations (HBD 1998).

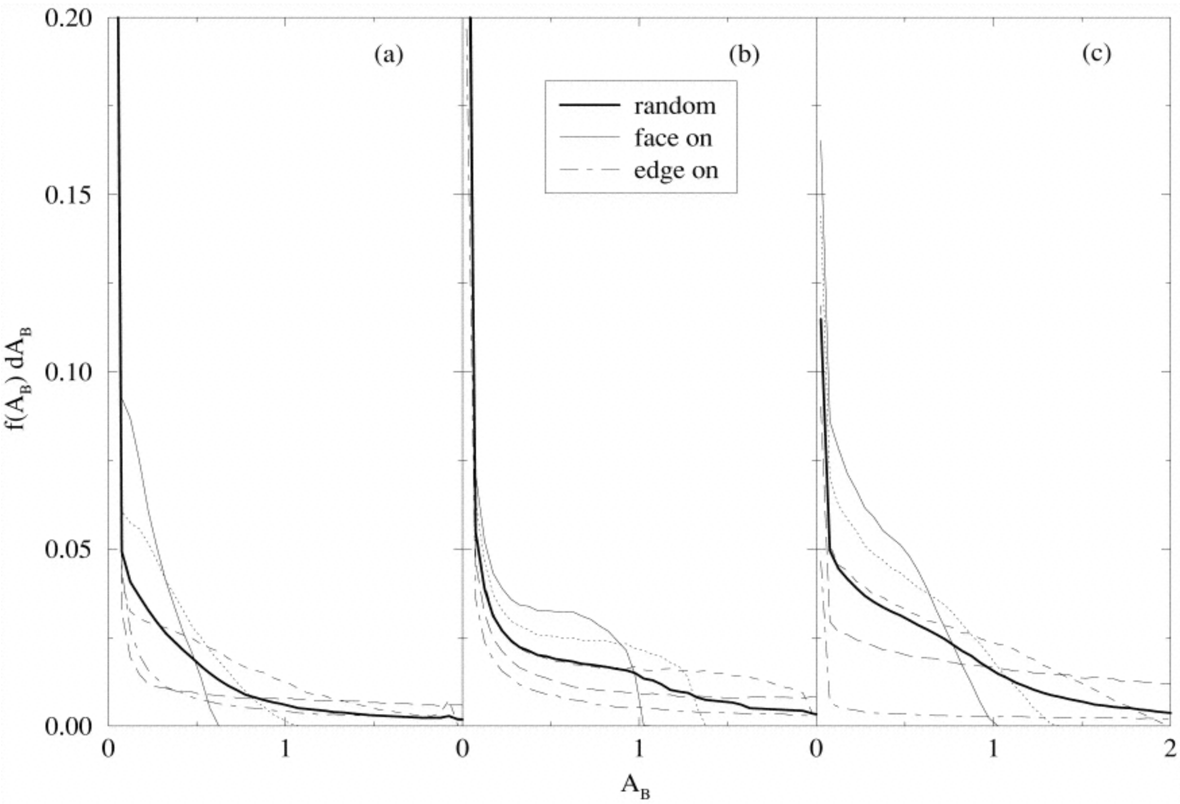

Figure 3: The probability for Ω_Λ based on the observed data. The probability is for each individual bin, of which 240 span the graph.

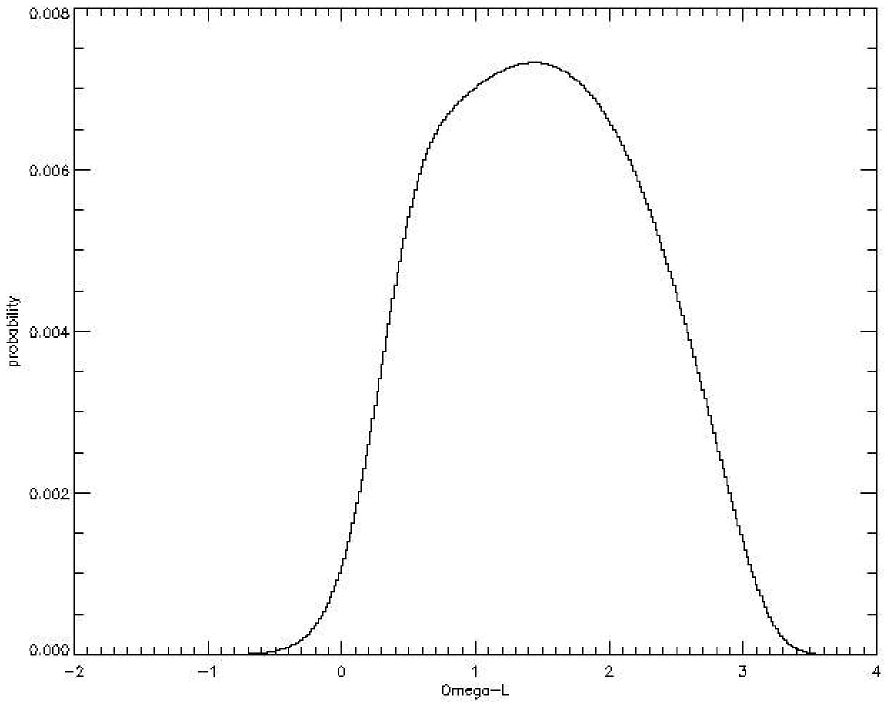

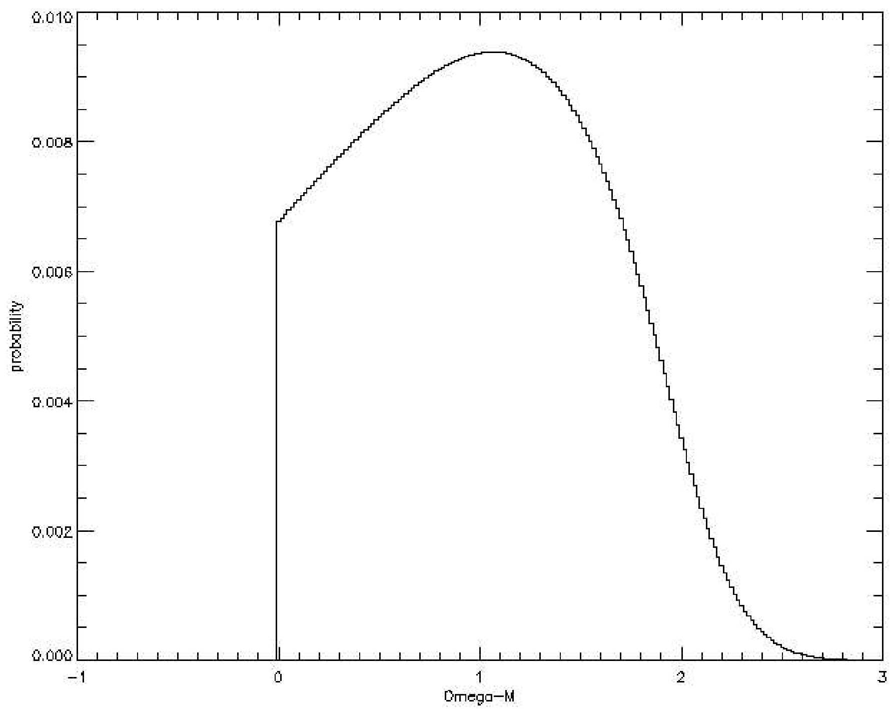

Figure 4: The probability function for Ω_M based on the data observed, with 180 bins

Figure 5: The probability density for $\mathcal{M}$ and α, primarily from low-z supernovae.

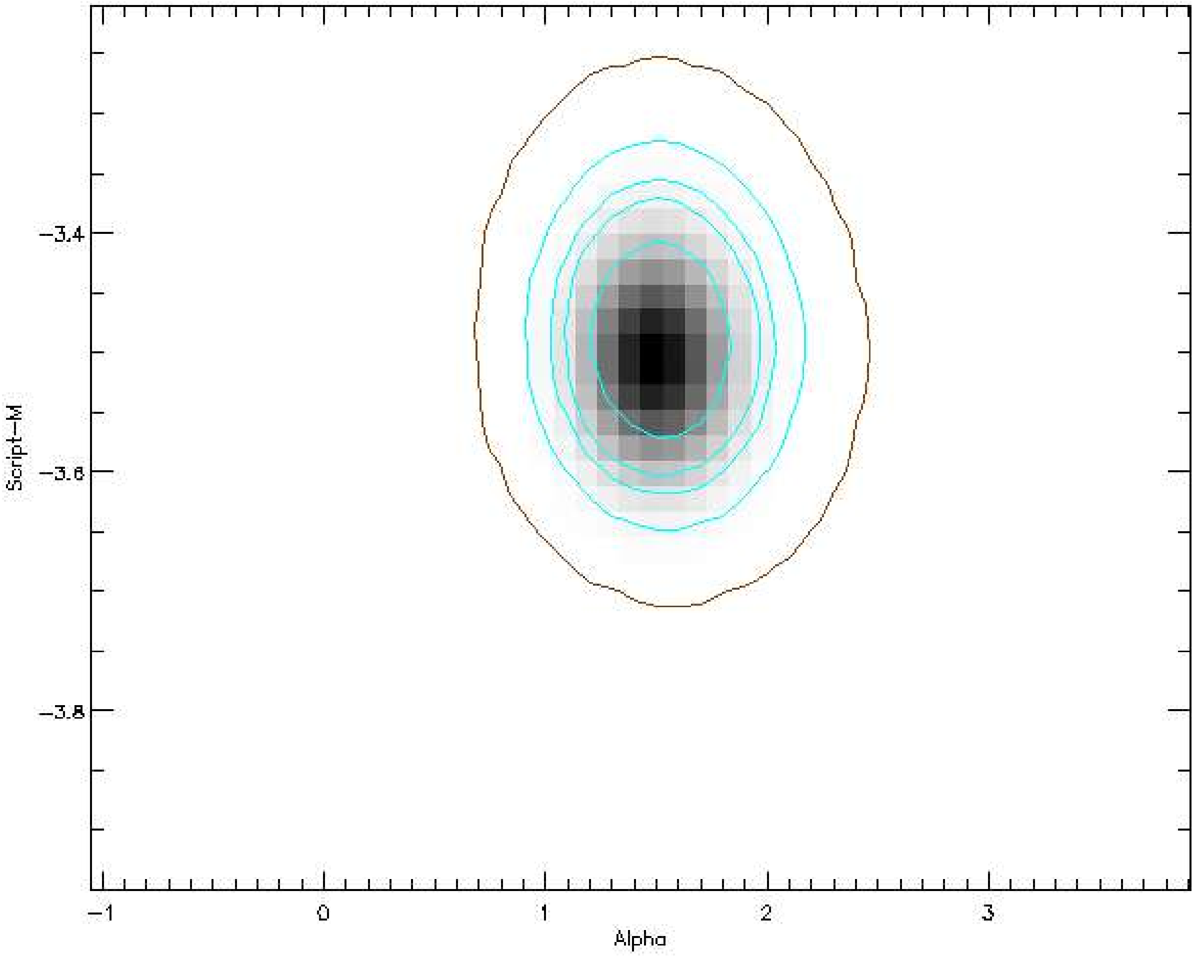

Figure 6: The k-corrected R band from z=0.7, with normalized peak flux allowed on the vertical axis and wavelength in angstroms on the horizontal axis. The peaks to the left and right of the corrected R-band are the rest-frame U- and B-bands.

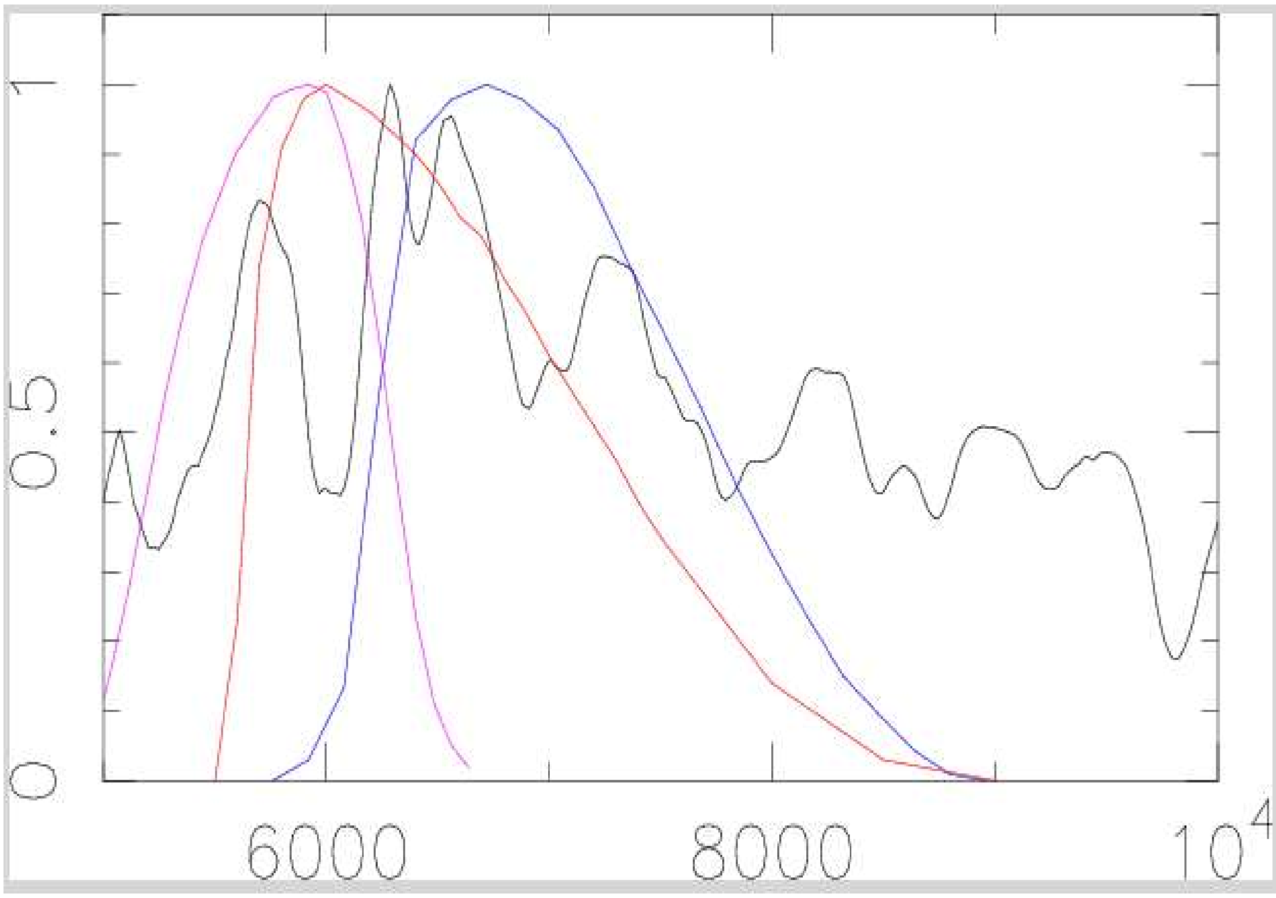

Figure 7: The confidence graph of Ω_M and Ω_Λ. Shown are the lines of 68%, 90%, 95%, 99% and 99.99% confidence. The lines below indicate an Ω_Λ =0 universe and a flat universe, with an extra line to show where the $\Omega_M = 0.3$, $\Omega_\Lambda = 0$ universe plotted in figure 9 would appear. It is easy to see that a flat universe is well within the errors on this graph.

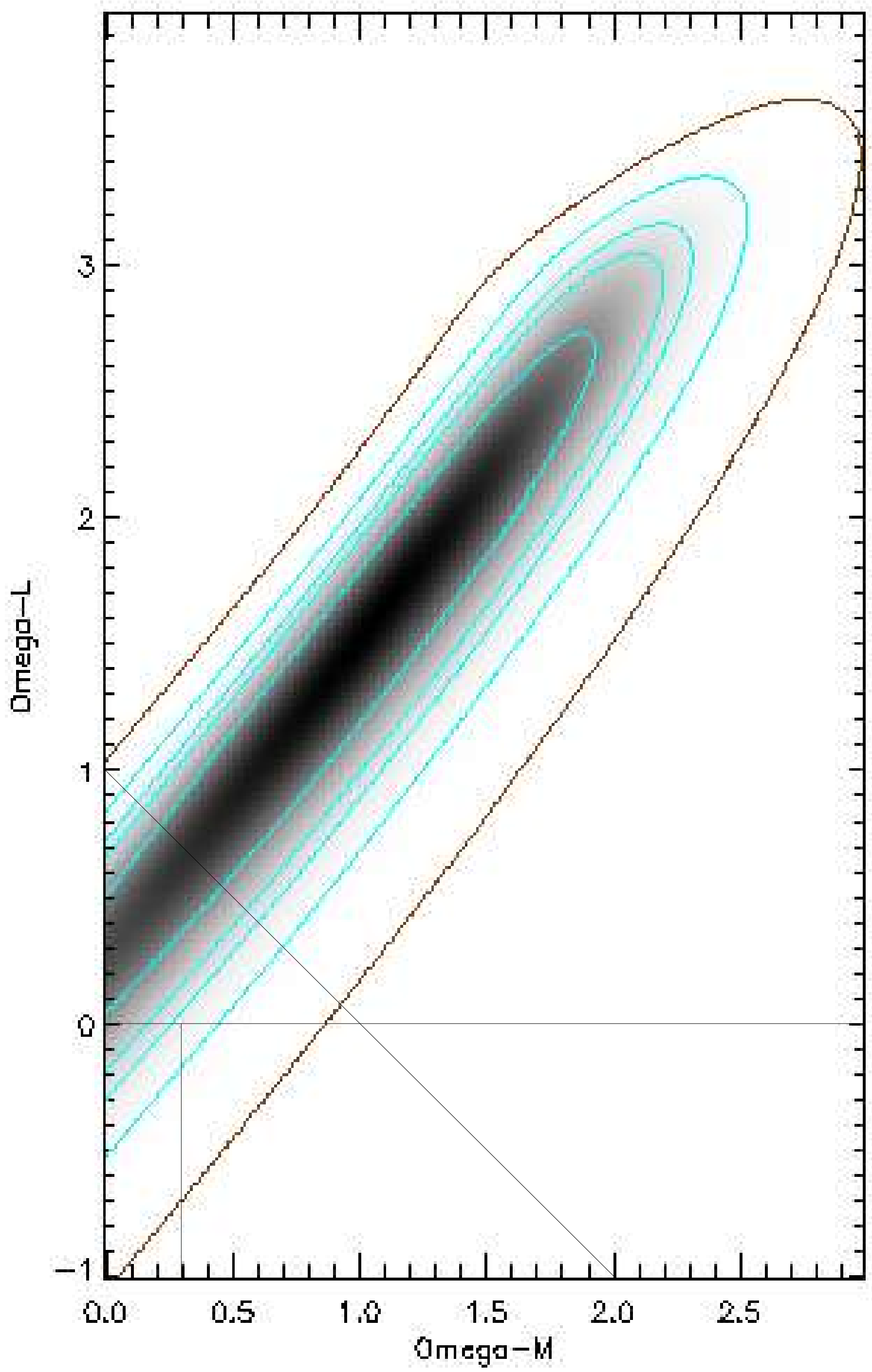

Figure 8: The probabilities of the values for Ω_M of each bin seen in figure 7 corresponding to a flat universe. This is essentially a cut of the probability density graph for the line $\Omega_M + \Omega_\Lambda = 1$.

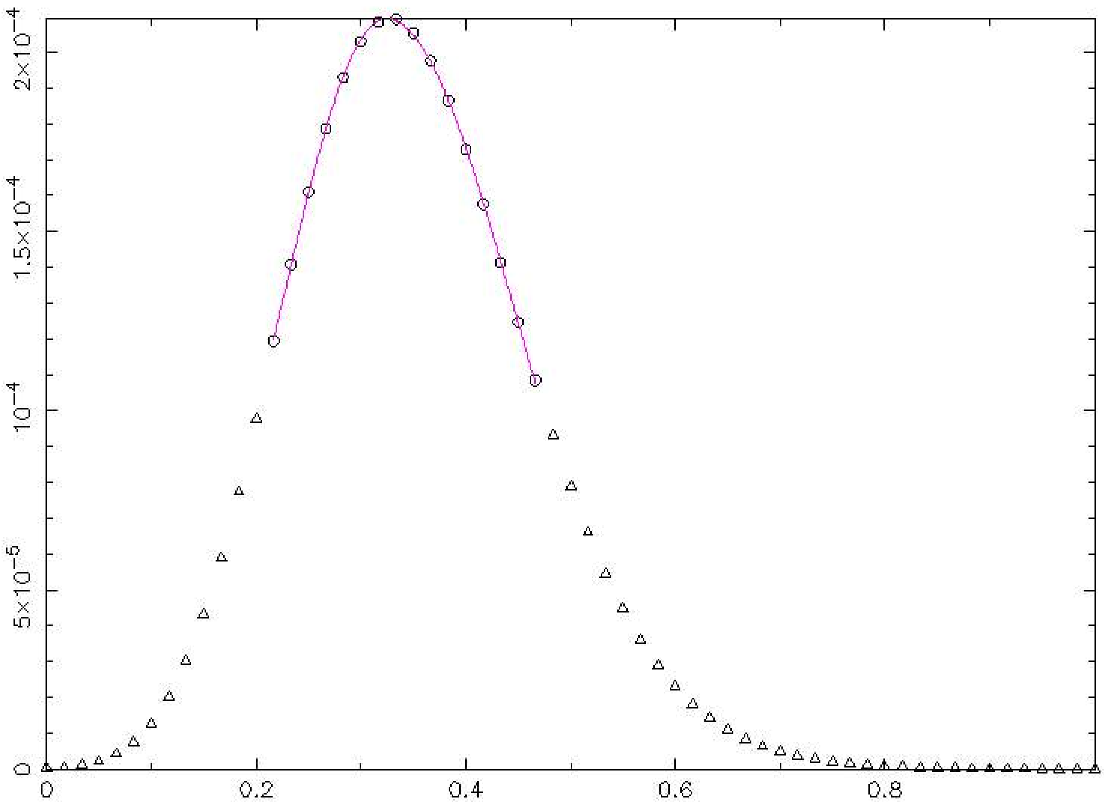

Figure 9: Effective B magnitude (stretch corrected) versus redshift for the 11 supernovae in this analysis. Three lines are shown, the solid line for Ω_M =0.3 and Ω_Λ =0.7, dashed for Ω_M =0.3 and Ω_Λ =0, and dotted for "Einstein-de-Sitter"